

Crack Propagation Quantification In Fibre-Reinforced Polymer Composites Through Distributed Optical Fibre Sensing

Koetsier, Mathieu; Pavlovic, Marko

Publication date

2024

Document Version

Final published version

Published in

Proceedings of the 21st European Conference on Composite Materials

Citation (APA)

Koetsier, M., & Pavlovic, M. (2024). Crack Propagation Quantification In Fibre-Reinforced Polymer Composites Through Distributed Optical Fibre Sensing. In C. Binetury, & F. Jacquemin (Eds.), *Proceedings of the 21st European Conference on Composite Materials: Volume 5 - Manufacturing* (Vol. 5, pp. 198-205). The European Society for Composite Materials (ESCM) and the Ecole Centrale de Nantes..

Important note

To cite this publication, please use the final published version (if applicable). Please check the document version above.

Copyright

Other than for strictly personal use, it is not permitted to download, forward or distribute the text or part of it, without the consent of the author(s) and/or copyright holder(s), unless the work is under an open content license such as Creative Commons.

Takedown policy

Please contact us and provide details if you believe this document breaches copyrights. We will remove access to the work immediately and investigate your claim.

CRACK PROPAGATION QUANTIFICATION IN FIBRE-REINFORCED POLYMER COMPOSITES THROUGH DISTRIBUTED OPTICAL FIBRE SENSING

Mathieu Koetsier¹ and Marko Pavlovic¹

¹Technical University Delft, Civil Engineering, Stevinweg 1, The Netherlands
Email: m.koetsier@tudelft.nl, Web Page: <https://www.tudelft.nl/staff/m.koetsier/>
Email: m.pavlovic@tudelft.nl, Web Page: <https://www.tudelft.nl/staff/m.pavlovic/>

Keywords: Delamination, Distributed Optical Fibre Technology, Structural Health Monitoring

Abstract

The progression of predictive models for crack propagation in fibre-reinforced polymer composites requires the quantification of crack development induced by both static and cyclic loading. The challenge of precisely measuring crack propagation becomes more intensified when cracks are not externally visible, such as in the case of delamination crack progression in thick composites. Traditional techniques, like 3D digital image correlation (3D DIC), can be employed to detect relative changes in strain distribution at the surface. However, these methods may prove insufficient, particularly for composite components with thicknesses ranging from 10mm to 100mm. Distributed optical fibre sensing emerges as a solution, enabling precise spatial measurement of strain along the fibre's length with a remarkable resolution of 0.65mm. Embedding fibres strategically in the composite during production allows measurements in close proximity to the crack surface. Placing fibres in the direction of crack growth facilitates the observation of changes in strain distribution, markedly enhancing the precision in quantifying the delaminated area compared to conventional surface monitoring methods. This investigation offers a comprehensive overview of the design, implementation, and experimental application in simple joint geometries. It places specific emphasis on large steel-glass fibre polymer composite bonded joints, commonly referred to as wrapped composite joints. The technique is initially applied to a straightforward wrapped splice joint with 1D crack propagation. The experimental results robustly affirm the effectiveness of the proposed monitoring system and postprocessing methods subjected to both static and cyclic loading conditions. The system and methods effectively quantify the propagation of debonding cracks. In summary, these findings underscore the achievability of accurately quantifying delamination crack propagation by embedding distributed optical fibres in thick composites. This study contributes valuable insights for the development of predictive models and strongly reinforces the practical significance of employing distributed optical fibre sensing in crack monitoring.

1. Introduction

Damage-tolerant designs in fibre-reinforced polymer structures during the service life are more common. This highlights the need for reliable predictive models [1], [2] and, consequently, for proper experimental data acquisition of the relevant failure mode. Challenges arise when failure modes, such as delamination cracks in thick fibre-reinforced polymer components, are not externally visible. Traditional techniques, like Digital Image Correlation (DIC), ultrasonics, X-rays or thermography, among others, have the advantage of detecting damage inside the composite, either direct or indirect [3], [4]. However, a trade-off is made in the accuracy of the monitoring technique when composite thicknesses increase from a few (1-5) mm to a couple (2-15) cm. More direct monitoring techniques like optical fibre sensors allow placement of the sensor near the expected damage. Optical fibres have attracted more attention for their potential in structural health monitoring (SHM), and a number of applications for damage detection in composites are reported [5]–[7]. Optical fibres can be utilized for

measuring; strain, temperature, pH, moisture, vibration and more. In this study, optical fibres are utilized as strain sensors. Utilizing strain measurements for damage detection requires the existence of a relation between damage and the strain field. Damage can be seen as a local change in the material properties leading to a change in structural response. Thus, the structure's response will change when damage initiates and propagates [4].

Several types of fibre optic sensing are available, grating-based sensors like fibre Bragg gratings (FBGs) and distributed sensing techniques utilizing Rayleigh or Brillouin scattering [8]. For a detailed description of the different sensor techniques, the reader is referred to an extensive review done by Di Sante [8]. In the current work, distributed strain sensing technique utilizing Rayleigh scattering is applied. The advantage of distributed strain sensing is that crack propagation can be monitored along the complete length of the optic fibre. By strategically orientating the fibres, a continuous monitoring system can be created.

For damage monitoring in thick composites (2-15cm), optical fibre sensors can be placed near the expected damage. Because of their limited diameter (125μ), they will not compromise the structural integrity. This study primarily focuses on investigating the feasibility of detecting delamination crack growth in composite wrapping, which serves as an alternative method for connecting circular hollow section (CHS) members. This innovative joining technique, known as wrapped composite joints, involves bonding steel and glass fibre polymer composite wrapping to facilitate load transfer. The predominant failure mode in such joints is debonding or delamination near the steel-composite interface [3], [9].

This work first presents the methodology of damage detection, explaining how strain sensing can be used to quantify damage during static failure experiments and cyclic crack growth experiments.

2. Methodology

The failure of joints utilizing bonding between adherents often manifests as debonding or delamination, with cracks propagating in the direction of the applied load. Throughout this failure process, the area responsible for transferring loads diminishes, leading to a redistribution of internal strain and stresses. A potential method for detecting this failure process involves measuring the redistribution of strain during crack propagation. This can be achieved by either measuring surface strains, as demonstrated by Feng & Pavlovic [3], or by employing optical fibres embedded within the composite. Surface strain measurements, while informative, exhibit limitations as the thickness of the composite increases. In contrast, optical fibres embedded within the composite do not face this limitation. However, strain measurements obtained from optical fibres are confined to the fibre's path, unlike surface strain measurements using DIC, which provide a broader view of strain distribution. In this study, the optical fibre is embedded inbetween the 2nd and 3rd ply from the steel-composite interface.

A virtual approach was adopted to simulate strain redistribution during crack propagation in splice joints to enhance experimental observations using finite element (FE) models. The specimen geometry is described in section 3.2. The 3D FE model shown in Figure 1 was developed using ABAQUS software [10], aligning with the design of tested specimens. Linear hexahedral eight-noded solid elements with reduced integration (C3D8R) are utilized to represent the steel components, ensuring accurate modelling of their mechanical behaviour. Conversely, linear tetrahedral elements (C3D4) are chosen for the composite due to their enhanced ability to capture complex geometries during meshing needed for more complex joints. Mesh sizes are aligned at the interface between the steel and composite materials. The interface behaviour between the composite and steel bond is characterized by a four-linear traction-separation law derived by [11]. An analysis of mesh size dependency is performed to assess its influence on strain distribution. Optimal results in terms of failure mode and ultimate resistance were achieved with a mesh size of 4mm on the steel and inside of the composite, and 8mm towards the outside of the composite. These FE models enable a systematic examination of strain distribution evolution with varying crack lengths, offering valuable insights into the behaviour of the joint under both static and cyclic loading conditions.

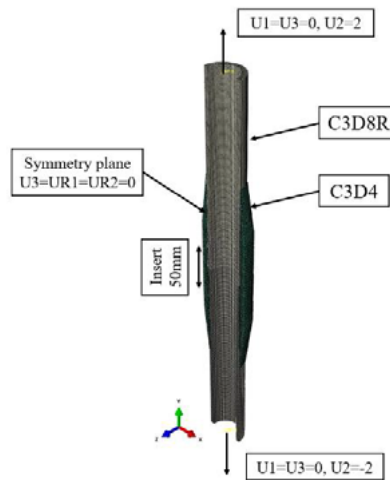


Figure 1. FE model.

2.1. Static crack growth

The static delamination process can be simulated using cohesive zone modelling (CZM), enabling observation of the strain distribution throughout the failure process. This comprehensive approach offers valuable insights into the evolution of delamination and its impact on strain distribution within the joint, thereby enhancing understanding of its structural behaviour. However, various factors influence this strain distribution, including delamination crack growth and increasing loads.

Figure 2a showcases the load-displacement curve derived from the FE model, providing insight into the force levels at which the longitudinal strain distributions are examined. On the other hand, Figure 2b portrays the strain associated with the onset of mode-II crack initiation, indicated with a dot, identified at the 20 MPa traction stress at the interface [11]. Subsequently, in Figure 3a, the corresponding strain distribution for each force level is illustrated, spanning from the initial force level of 195kN to the final force level of 844kN, representing the fully developed slip at the initial crack tip. An observable trend emerges in the strain distribution as the force increases. Overall strain levels rise due to crack progression towards the wrapping end and the accompanying increase in force. To mitigate the influence of increasing load on strain distribution, consideration can be given to the relative change in strain distribution to eliminate the interference of elastic strain. This involves scaling the strain to a reference force level representing a pure elastic loading stage, assuming a linear dependence between strain and force. Figure 3b demonstrates this approach, where the initiation force serves as the reference force level. Strains at subsequent load stages are scaled to this reference force. Without damage or crack growth, the scaled strain remains unchanged compared to the reference force level. This ensures that any deviation in the scaled strain is solely attributable to the progression of delamination cracks, thereby isolating its relative change in strain distribution. It is crucial to select the reference force level carefully to ensure it represents a state of the joint where no nonlinear behaviour has occurred. Therefore, the load level corresponding to the initiation of the crack based on the CZM is suggested as a suitable reference force level.

The FE technique serves to establish a relationship between the scaled strain distribution and the length of delamination cracks. At each stage of the analysis, the crack length is precisely determined, with the crack tip located at the point of crack initiation, as evidenced by the termination of the linear section of the cohesive zone model (CZM) for mode-II fracture. In Figures 3a and b, vertical lines indicate the position of the crack tip. It is noteworthy that in Figure 3a, the strain at the crack tip exhibits a slight increase as the crack advances, potentially attributed to the increase in load level. Conversely, in Figure

3b, a decrease in the scaled strain at the crack tip is observed, eventually stabilizing. This decrease corresponds to the development of the full fracture process zone, with the stable scaled strain level being attained upon the completion of this process and the subsequent progression of the crack.

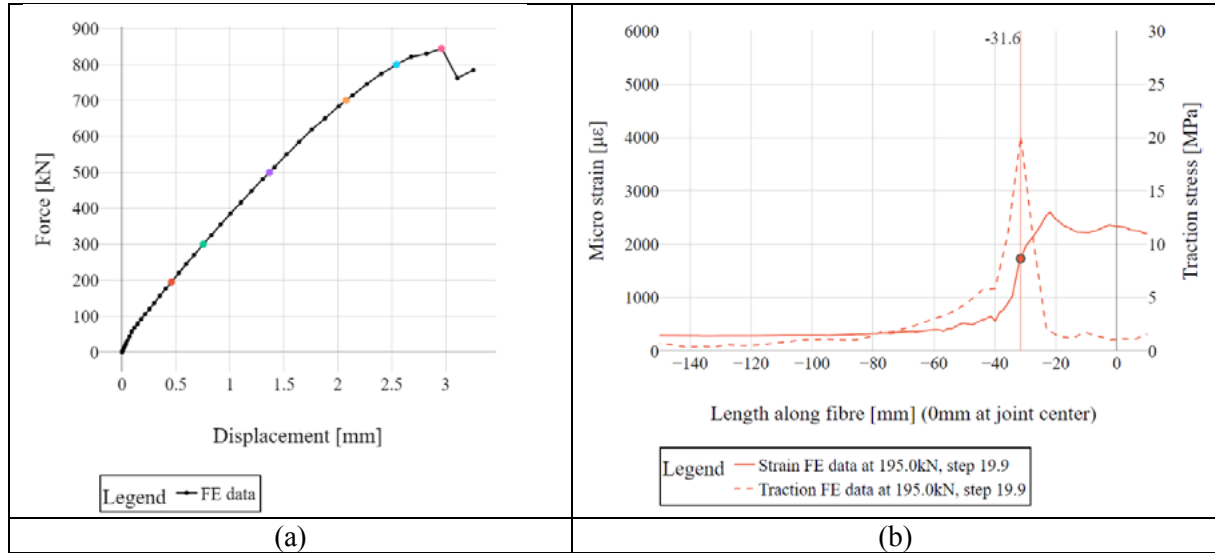


Figure 2. a) Force displacement curve static FE simulation. b) Microstrain and traction at the onset of initiation

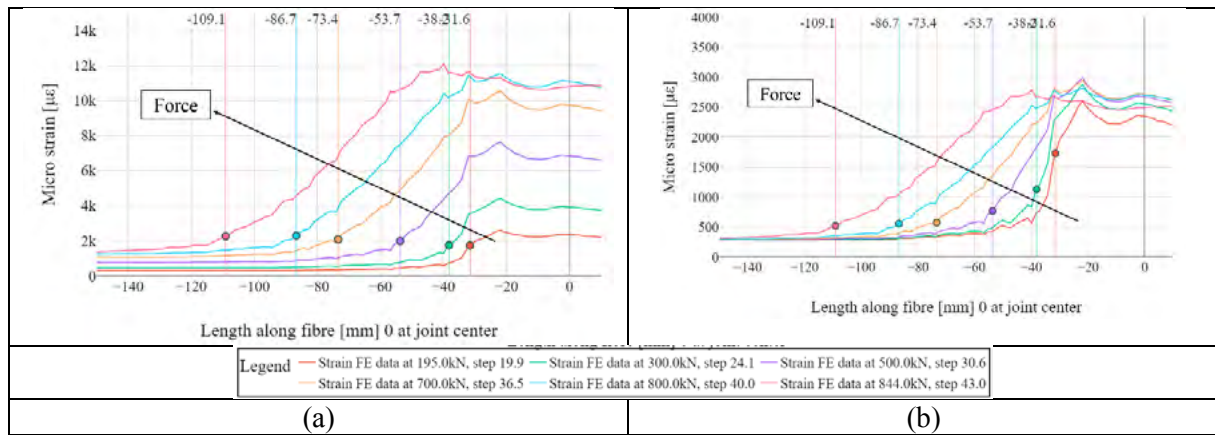


Figure 3. a) microstrain along fibre path obtained from FE model. b) microstrain along fibre path obtained from FE model scaled by force ratio to 195kN.

2.2. Cyclic crack growth

During cyclic loading, the delamination crack propagates with each cycle, resulting in changes in the strain distribution. Unlike static strain distribution, cyclic strain distribution is consistently measured at a similar load level in force-controlled experiments. During experimental observations, the strain range is determined between the minimum and maximum load; the strain range allows to mitigate the effects of temperature fluctuations and creep. Similarly, the strain readings from the FE model are transformed to the strain range. Multiple analyses are conducted with different crack lengths to provide insight into the redistribution of longitudinal strain induced by cyclic crack propagation.

Figure 4 presents the associated longitudinal strain range from the joint centre to the wrapping end for multiple delamination lengths. The strain range is determined to fall between 33 and 330kN. Notably, the strain plateau at approximately 4000 microstrain extends as the crack progresses. Similar to the determination of the static crack tip, the 20MPa traction at the interface is utilized to quantify the crack tip. It is evident that the fracture process zone develops at this load level, resulting in a crack length larger than the initial debonding length in the FE model. As expected, the strain level at the crack tip remains constant as the crack progresses. This suggests that a constant strain threshold can be employed for fatigue crack detection by optical fibres.

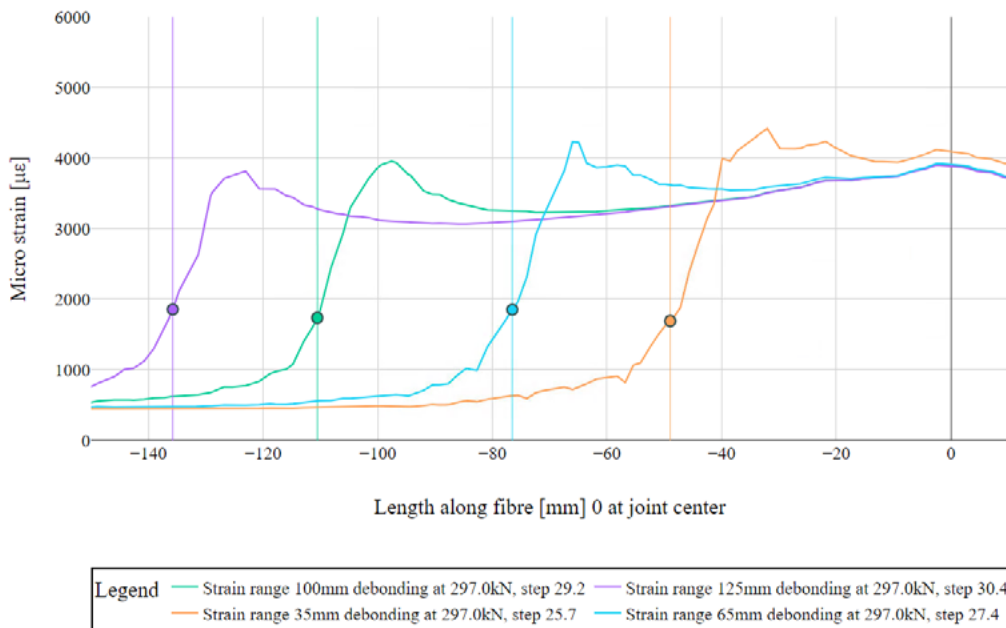


Figure 4. Microstrain along fibre path obtained from FE model for multiple initial debonding lengths.

3. Experimental tests and results

The experimental investigation comprises static and cyclic tests performed on steel-to-composite bonded joints, referred to as "wrapped joints." These tests encompassed splice joints, which connect two steel tubular circular hollow sections (CHS). Initially, section 3.1 offers an overview of the types of optical fibre sensors used and their implementation. Following this, section 3.2 presents the experimental results.

3.1 Sensor preparation

Luna ODISI 6000 [12] is employed in conjunction with Omocer-coated glass fibre from FBGS [13]. The Omocer-coated fibre is selected for its high strain at break and high reflection index. In the joint production process, optical fibres are embedded inside the composite wrap near the interface according to the applied pattern depicted in Figure 6a. During the wrapping process, initially, 2 plies of glass-fibre composite are applied, followed by the placement of the optical fibres. Subsequently, the remaining composite is wrapped, with a thickness of 15mm.

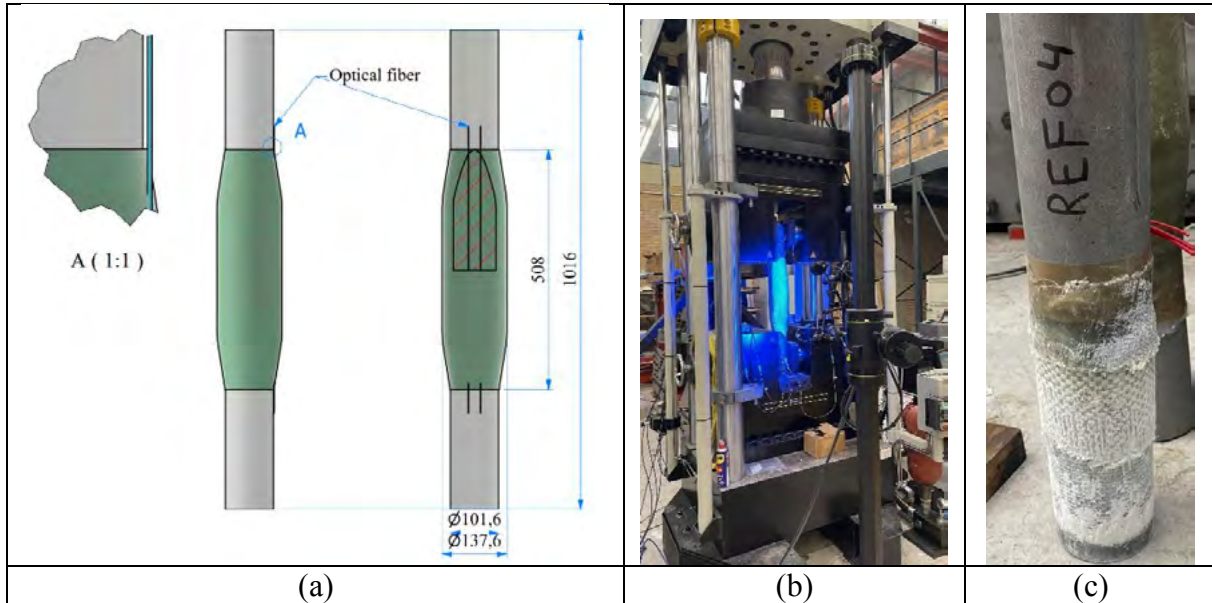


Figure 5. a) Optical fibre pattern in wrapped splice joint. b) Photo of test setup. c) Photo of failure surface.

3.2 Splice joint

The experimental setup involves testing simplified splice-wrapped joints that connect two tubular tubes of $\varnothing 101.6 \times 10$ mm under both fatigue and static loading conditions. The testing protocol comprises two primary steps: first, initiating and growing a fatigue delamination crack near the interface to a predetermined length of approximately 101 mm, followed by subjecting the joints to static loading until failure to assess their static resistance post-fatigue. These tests are conducted using an Instron 8806 testing machine, see Figure 5b. For cyclic loading, a force ranging from 33 kN to 330 kN is applied at a frequency of 2 Hz, while static tests are performed under displacement control with a jack displacement rate of 0.5 mm/min. Optical fibre measurements are collected during both cyclic and static loading phases, with readings taken at force levels of 30 kN and 330 kN during cyclic loading at an interval of 500 to 1000 cycles and at regular intervals during static loading ranging from 5 to 1 second, gradually increasing towards the failure load. A delamination type of failure mode near the steel to composite is observed in these experiments as depicted in Figure 5c.

Figure 6a illustrates the stiffness degradation observed during the fatigue loading of the splice joint. Each dot in the graph represents the visualized microstrain range presented in Figure 6b. A similar trend is observed in the experimental results as in the FE approach described earlier. Specifically, the strain plateau extends as the crack progresses. Based on the microstrain range obtained from the FE analysis, as shown in Figure 4, the strain range at the crack tip is approximately 1900 microstrain. By employing this threshold, the relationship between crack length and cycles can be determined (see Figure 6a).

Figure 7 displays the load-displacement curve depicting the static resistance following fatigue testing. Important to note here is that different from the FE results, a fatigue crack has already been developed. The representative load levels corresponding to optical fibre strain readings, shown in Figure 8, are marked. Analysis of Figure 8a suggests an initial increase in absolute strain at the delaminated area during loading. However, upon scaling the strain readings to a reference force of 195 kN, as illustrated in Figure 8b, a distinct transition is observed as delamination progresses. It can be seen that crack propagation initiates between points 3 and 4.

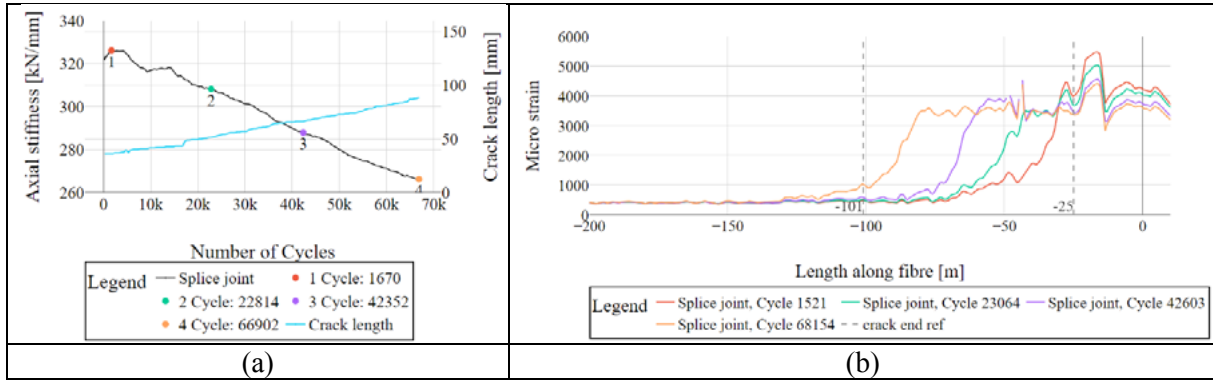


Figure 6. a) Stiffness degradation cyclic splice joint. b) Microstrain range from optical fibre measurements at 1670, 22814, 42352 and 66902 cycles.

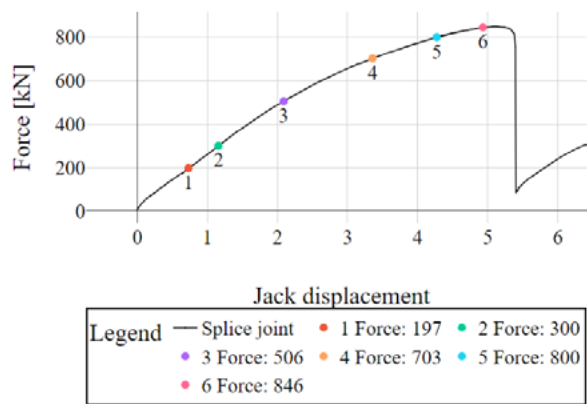


Figure 7. Load-displacement static after fatigue with indication load levels of strain reading

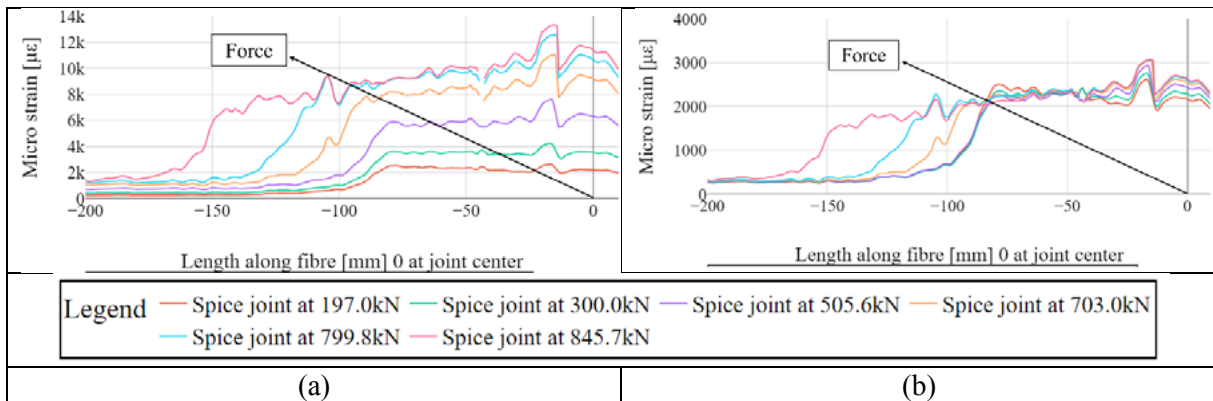


Figure 8. Microstrain along fibre path a) from the experiment. b) obtained from scaling by force ratio to 195kN.

3. Conclusions

This study investigated the fracture behaviour of simple bi-material bonded joints, with a specific emphasis on monitoring mode II delamination crack propagation. Through numerical and experimental approaches, insight was gained into the evolution of delamination and its impact on strain distribution. Both numerical and experimental strain readings near the delamination surface provided comprehensive results. Finite element modelling was instrumental in establishing a correlation between strain distributions and delamination crack lengths. A strain scaling method was proposed to exclude the linear

relationship between strain and load. This scaled strain distribution revealed a dependency of the strain level at the crack tip and the fracture process. During forming of the fracture process, the strain at the crack tip reduces and stabilizes upon full development of the fracture process zone. Indicating that a constant threshold is not representative for crack development phase.

Optical fibre measurements conducted during both static and cyclic experiments demonstrated good agreement with numerical models. Optical fibre measurements emerged as a suitable method for accurately measuring delamination lengths. However, the selection of a threshold strain value at the crack tip should be carefully determined in conjunction with FE analysis.

Acknowledgments

The authors would like to express their gratitude to RVO for the financial support with Topsector Energiesubsidie van het Ministerie van Economische Zaken through WrapNode-I project, and Tree Composites B.V. for the production of specimens.

References

- [1] T. K. O'Brien, "Towards a Damage Tolerance Philosophy for Composite Materials and Structures," *Composite Materials: Testing and Design (Ninth Volume)*, vol. STP1059-EB. ASTM International, p. 0, Jan. 01, 1990. doi: 10.1520/STP24105S.
- [2] T. E. Tay, G. Liu, V. B. C. Tan, X. S. Sun, and D. C. Pham, "Progressive Failure Analysis of Composites," *J. Compos. Mater.*, vol. 42, no. 18, pp. 1921–1966, Jul. 2008, doi: 10.1177/0021998308093912.
- [3] W. Feng and M. Pavlovic, "Fatigue behaviour of non-welded wrapped composite joints for steel hollow sections in axial load experiments," *Eng. Struct.*, vol. 249, p. 113369, Dec. 2021, doi: 10.1016/J.ENGSTRUCT.2021.113369.
- [4] A. Güemes, A. Fernández-López, P. F. Díaz-Maroto, A. Lozano, and J. Sierra-Perez, "Structural health monitoring in composite structures by fiber-optic sensors," *Sensors (Switzerland)*, vol. 18, no. 4, pp. 1–11, 2018, doi: 10.3390/s18041094.
- [5] K. S. C. Kuang, S. T. Quek, C. G. Koh, W. J. Cantwell, and P. J. Scully, "Plastic optical fibre sensors for structural health monitoring: A review of recent progress," *J. Sensors*, vol. 2009, 2009, doi: 10.1155/2009/312053.
- [6] B. Hofer, "Fibre optic damage detection in composite structures," *Composites*, vol. 18, no. 4, pp. 309–316, 1987, doi: 10.1016/0010-4361(87)90294-1.
- [7] J. Palaniappan, "University of Surrey," University of Surrey, 2008. doi: 10.1111/j.1468-0270.1989.tb01141.x.
- [8] R. Di Sante, "Fibre optic sensors for structural health monitoring of aircraft composite structures: Recent advances and applications," *Sensors (Switzerland)*, vol. 15, no. 8, pp. 18666–18713, 2015, doi: 10.3390/s150818666.
- [9] P. He and M. Pavlovic, "Failure modes of bonded wrapped composite joints for steel circular hollow sections in ultimate load experiments," *Eng. Struct.*, vol. 254, p. 113799, Mar. 2022, doi: 10.1016/J.ENGSTRUCT.2021.113799.
- [10] D. S. S. Corp., "Abaqus Unified FEA - SIMULIA." Dassault Systèmes, 2023.
- [11] P. He, "Debonding Resistance of CHS Wrapped Composite X-Joints," Delft University of Technology. doi: <https://doi.org/10.4233/uuid:3ad94ee9-07fd-47f9-a766-843a91830534>.
- [12] L. I. Incorporated, "ODISI 6000 Optical Sensor Interrogation System." Luna Innovations Incorporated, 2023. [Online]. Available: <https://lunainc.com/products/odisi-6000-optical-sensor-interrogation-system>
- [13] "Strain Sensing - FBGS." <https://fbgs.com/solutions/strain-sensing/> (accessed Nov. 28, 2023).